

Synthesis and Phase Structures of Mesogen-Jacketed Liquid Crystalline Polyelectrolytes and Their Ionic Complexes

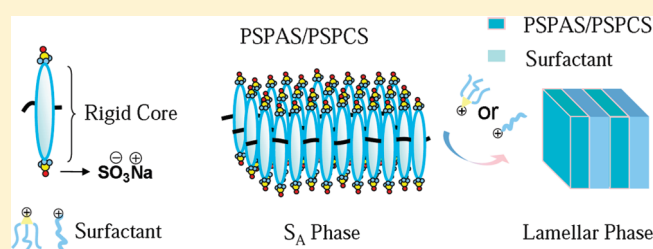
Yan-Hua Cheng,^{†,‡} Wen-Ping Chen,[‡] Cui Zheng,[†] Wei Qu,[†] Hongliang Wu,[†] Zhihao Shen,^{*,†} Dehai Liang,[†] Xing-He Fan,^{*,†} Mei-Fang Zhu,^{*,‡} and Qi-Feng Zhou[†]

[†]Beijing National Laboratory for Molecular Sciences, Key Laboratory of Polymer Chemistry and Physics of Ministry of Education, College of Chemistry and Molecular Engineering, Peking University, Beijing 100871, China

[‡]State Key Laboratory for Modification of Chemical Fibers and Polymer Materials, Donghua University, Shanghai 201620, China

 Supporting Information

ABSTRACT: Two mesogen-jacketed liquid crystalline polyelectrolytes, poly{sodium 2,5-bis[(4-sulfophenyl)aminocarbonyl]-styrene} and poly{sodium 2,5-bis[(4-sulfophenyl)oxycarbonyl]-styrene}, with rigid cores containing different linkages at the center and sulfonate groups on the two ends in the side chains were designed and successfully synthesized via conventional radical polymerization. X-ray scattering experiments revealed that the two polymers exhibited smectic A phases in bulk. Comb-shaped nonstoichiometric polymer–surfactant complexes were obtained by mixing the anionic sulfonated polyelectrolytes and cationic lipids of different lengths and shapes. The formation of ordered structures of the complexes depended on the length and shape of the lipids. Lamellar phases were observed when the two polyelectrolytes complexed with cetyltrimethylammonium bromide and fan-shaped 3,4,5-tris(dodecyloxy)benzenamine. Owing to the stronger bond strength of electrostatic interactions, the types of mesophases of the complexes based on the two polyelectrolytes with different linkages in the rigid cores were the same.



INTRODUCTION

In an attempt to mimic biological systems, construction of self-assembled complex functional systems with ordered structures is preferentially performed following the rules of supramolecular chemistry based on secondary interactions, such as ionic interactions and hydrogen bonding rather than covalent bonding.^{1,2} Compared with hydrogen bonding, ionic interactions have stronger bond strength.³ Because of the facile synthesis and broad applications of ionic complexes, various polyelectrolyte architectures, such as linear, hyperbranched, and dendronized, have been used as polybases. When they complex with oppositely charged surfactants, the resulting complexes have been shown to form microphase-separated morphologies,^{2,4–8} which influence the surface, optoelectronic, and mechanical properties.^{9–11}

Rigid-rod polyelectrolytes are rich in living organisms. They have great abilities to form specific well-ordered structures by spontaneous self-assembly and play an important role in the normal function of lives.^{12–14} In order to study the mechanisms and properties of these biopolyelectrolytes in living organisms, recent efforts have been focused on the synthesis of rigid-rod liquid crystalline (LC) polyelectrolytes and the investigation of their properties in solutions and in bulk.^{15–19} In our previous study, we have systematically investigated a special type of side-chain LC polymers, mesogen-jacketed liquid crystalline polymers (MJLCPs), which have a short spacer or a single bond between the attached side-on side chains and the polymer backbone. MJLCPs behave like a rigid rod because of the

“jacketing” effect. They can be easily synthesized by radical polymerizations, and their physical characteristics can be tuned by controlling the chemical structures of the side chains.²⁰ Smectic phases have also been reported in MJLCPs when the length (or the rigidity) of the mesogen is increased,²¹ or when semifluorinated tails are used,²² or when hydrogen bonding is introduced into the mesogens.²³ To better elucidate the mechanism of self-organizing behavior of biopolyelectrolytes, it is meaningful to design and study LC properties of a special type of polyelectrolytes based on the MJLCP model.

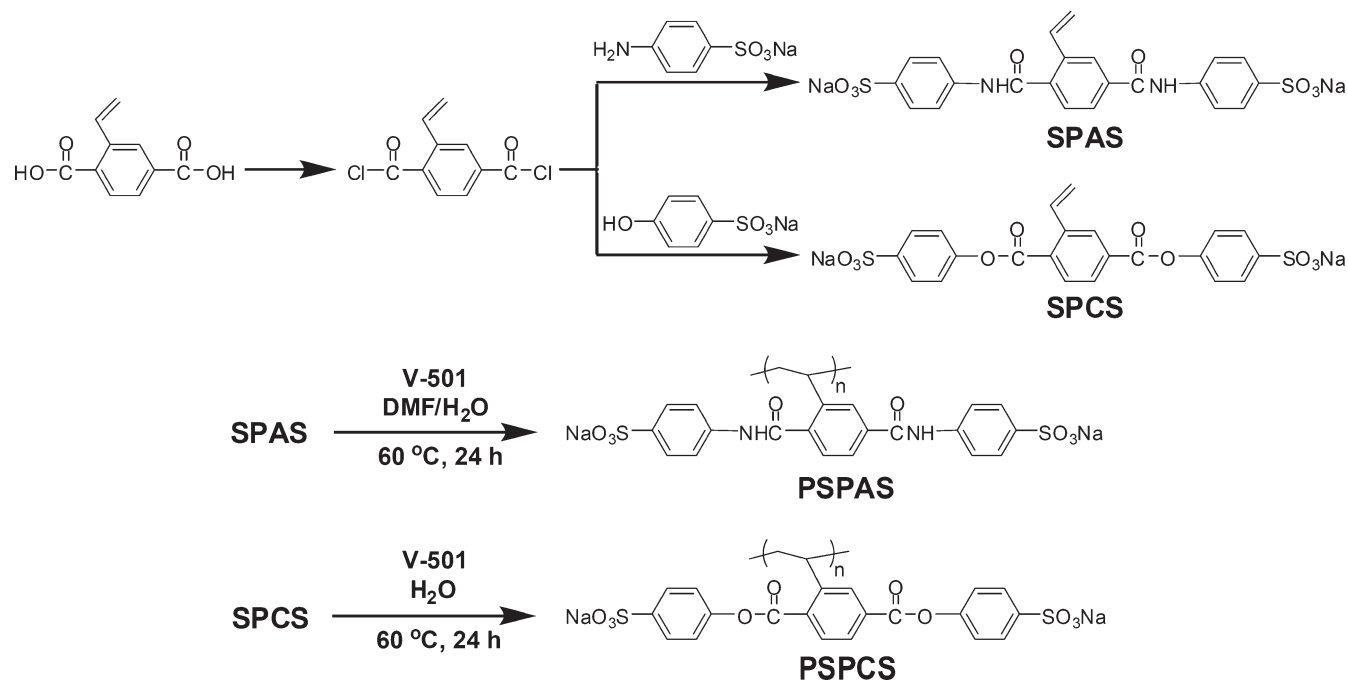
In this work, we report for the first time the design and synthesis of a new series of sulfonated mesogen-jacketed liquid crystalline polyelectrolytes (MJLCPs), in which the attached mesogens had a rigid core containing amide or ester linkages, with sulfonated groups appended on the two ends of the core. The self-assembly and LC structures of the MJLCPs in bulk were investigated using various techniques. Furthermore, ionic moieties were introduced into the side chains of the MJLCPs by forming complexes between the anionic MJLCPs and cationic surfactants. The effects of MJLCP structure, alkyl tail length, and surfactant shape on liquid crystalline structures of the complexes were investigated.

Received: January 15, 2011

Revised: April 15, 2011

Published: April 28, 2011

Scheme 1. Synthetic Routes of Monomers and Polyelectrolytes



EXPERIMENTAL SECTION

Materials. The compound vinylterephthalic acid was synthesized using the method reported previously.²⁴ 4,4'-Azobis(4-cyanovaleric acid) (V-501, Aldrich) was used as received. *N,N'*-Dimethylformamide (DMF, Beijing Chemical Co., A.R.) was distilled over CaH₂ prior to use. Acetone was refluxed over potassium permanganate and distilled out, followed by drying with anhydrous calcium sulfate powder and distilling out before use. All other reagents and solvents were used as received from commercial sources.

Measurements. ¹H NMR spectra were obtained using a Bruker ARX400 MHz with tetramethylsilane (TMS) as the internal standard at ambient temperature in dimethyl-*d*₆ sulfoxide and methanol-*d*₄. Mass spectra were recorded on a Bruker Apex IV FTMS spectrometer.

Polarized light microscopy (PLM) was used to observe the LC textures of the samples on a Leitz Laborlux 12 microscope. The images were captured using an insight digital camera. The film was prepared by solution-casting from water. The specimens were slightly sheared from concentrated solutions to increase the LC domain size.

Dynamic light scattering (DLS) and static light scattering (SLS) were conducted on a commercialized spectrometer from Brookhaven Instruments Corp. in a scattering angular range of 20°–120° at 25 °C. A solid-state laser polarized at the vertical direction (CNI Changchun GXC-III, 532 nm, 100 mW) operating at 532 nm was used as the light source.

Viscosities of PSPAS and PSPCS were measured in water solutions at 30 °C with an Ubbelohde capillary viscometer.

Small-angle X-ray scattering (SAXS) experiments were performed using a SAXSess instrument (Anton Paar) equipped with a Kratky block-collimation system. The X-ray was generated using a Philips PW3080 sealed-tube X-ray generator with the Cu target. The wavelength was 0.1542 nm. A highly sensitive SAXS imaging plate which was 264.5 mm away from the sample was used to collect the signal in vacuum. Samples were placed in between aluminum foils which were folded and sandwiched in a steel sample holder. Scattering data were acquired for a 30 min exposure. The background scattering from aluminum foils was acquired and then subtracted from the sample profiles.

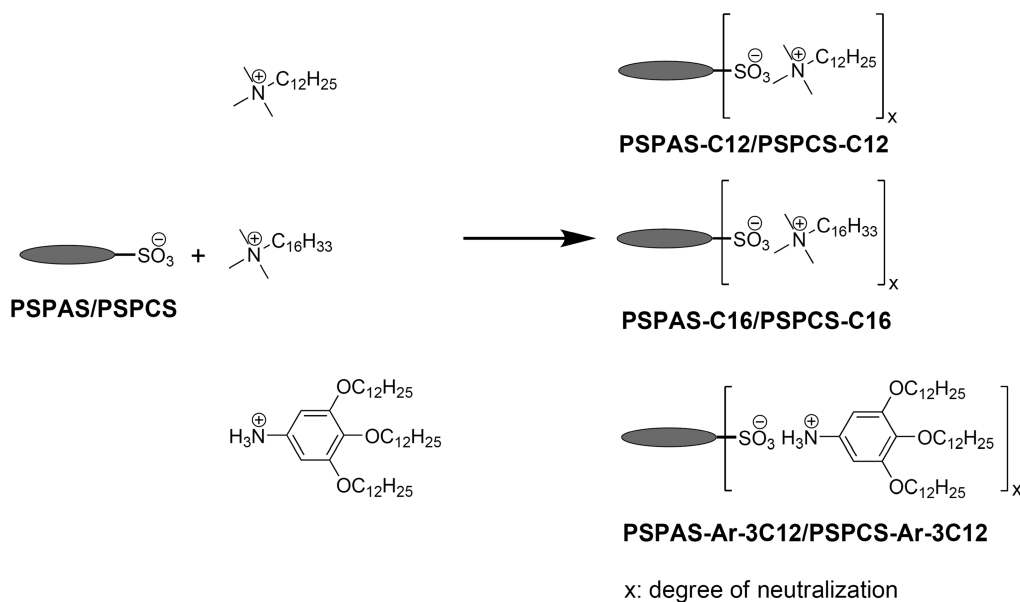
Two-dimensional (2D) wide-angle X-ray diffraction (WAXD) experiments were performed on a Bruker D8Discover diffractometer with GADDS as a 2D detector. The 2D diffraction patterns were recorded in a transmission mode at ambient temperature. The background scattering was recorded and subtracted from the sample patterns.

All time-resolved FTIR spectra were collected on a Nicolet 8700 FTIR spectrometer with a resolution of 4 cm⁻¹, 32 scans coadded for each spectrum, and the samples were mixed with KBr and then pressed into thin transparent disks.

Synthesis of Sulfonated Monomers. The synthesis of the monomers, sodium 2,5-bis[(4-sulfophenyl)aminocarbonyl]styrene (SPAS) and sodium 2,5-bis[(4-sulfophenyl)oxycarbonyl]styrene (SPCS), followed the method described in the literature.²⁵ The synthetic routes of SPAS and SPCS are shown in Scheme 1. The experimental details of the monomer synthesis and characterization are described below using SPAS as an example.

Synthesis of Sodium 2,5-Bis[(4-Sulfophenyl)aminocarbonyl]styrene (SPAS). Vinylterephthalic acid (2.4 g, 12.5 mmol), 20 mL oxalyl chloride, and a few drops of DMF were dissolved in dichloromethane (30 mL) in a 50 mL round-bottom flask. The mixture was stirred for 5 h. After evaporation of the solvent under reduced pressure, the residue was dissolved in anhydrous acetone. The resultant light yellow solution of vinylterephthal chloride was slowly dropped into an intensely stirred mixture of 25 mL of saturated brine aqueous solution and sodium 4-aminobenzenesulfonate (4.88 g, 25 mmol) in an ice/water bath and stirred for 15 min. Then saturated NaHCO₃ (30 mL) was added to the residue, and the reaction mixture was further stirred for 20 min. After SPAS was separated out, it was washed with DMF and recrystallized from methanol/H₂O (5/1, v/v) to give the product as a pale yellow solid. ¹H NMR (400 MHz, DMSO-*d*₆, δ, ppm): 5.46 (d, 1H, =CH₂), 6.05 (d, 1H, =CH₂), 6.96–7.03 (q, 1H, -CH=), 7.58–7.80 (m, 9H, Ar-H), 7.99 (d, 1H, Ar-H), 8.34 (s, 1H, Ar-H), 10.54 (s, 1H, -NH-), 10.62 (s, 1H, -NH-). ¹³C NMR (100 MHz, DMSO-*d*₆, δ, ppm): 117.73, 118.73, 119.53, 124.59, 126.05, 126.14, 126.93, 127.69, 133.25, 134.93, 135.84, 138.63, 139.06, 143.70, 164.69, 166.83. Anal. Calcd for C₂₂H₁₆N₂Na₂O₈S₂ (%): C 48.35, H 2.95, N 5.13. Found (%):

Scheme 2. Preparation of the MJLCPE–Surfactant Complexes



C 48.15, H 3.17, N 5.06. HRMS (ESI) m/z Calcd, $[M + H]^+$, 547.0216. Found, 547.0208.

Synthesis of Sodium 2,5-Bis[(4-Sulfophenyl)oxycarbonyl]-styrene (SPCS). SPCS was similarly prepared as mentioned for SPAS. ^1H NMR (400 MHz, $\text{DMSO}-d_6$, δ , ppm): 5.54 (d, 1H, = CH_2), 5.95 (d, 1H, = CH_2), 7.29 (d, 4H, Ar–H), 7.39–7.46 (q, 1H, –CH=), 7.73 (d, 4H, Ar–H), 8.19–8.26 (m, 2H, Ar–H), 8.39 (s, 1H, Ar–H). ^{13}C NMR (100 MHz, $\text{DMSO}-d_6$, δ , ppm): 119.11, 121.19, 127.01, 128.06, 128.85, 131.15, 132.03, 132.60, 133.95, 139.14, 146.24, 146.29, 150.28, 150.42, 163.79, 164.68. Anal. Calcd for $\text{C}_{22}\text{H}_{14}\text{Na}_2\text{O}_{10}\text{S}_2$ (%): C 48.18, H 2.57. Found (%): C 48.01, H 2.77. HRMS (ESI) m/z Calcd, $[M + \text{Na}]^+$, 570.9716. Found, 570.9704.

Polymerization of MJLCPEs. As shown in Scheme 1, the MJLCPE polymers were obtained by conventional radical polymerization in solution. A typical polymerization procedure was carried out as the following using PSPAS as an example. SPAS (0.5 g, 0.46 mmol), 100 μL of DMF solution of 0.02 M V-501, and 9.5 mL of DMF/water (2/1, v/v) were transferred into a polymerization tube. After three freeze–pump–thaw cycles, the tube was sealed off under vacuum. Polymerization was carried out at 60 °C for 24 h. The tube was then opened, and the reaction mixture was diluted with 10 mL of water. The resultant polymer was precipitated and washed with a mixed solvent methanol/water (5/1, v/v). To completely eliminate the unreacted monomer, the precipitate was redissolved in water and then reprecipitated in methanol/water (5/1, v/v) for three times. The absence of the monomer in the product was confirmed by thin-layer chromatography. Finally, the polymer PSPAS was dried in vacuum at 60 °C for 72 h. The polymerization method for PSPCS was similar to that for PSPAS, except that the polymerization solvent for PSPCS was pure water.

Preparation of MJLCPE–Surfactant Complexes. Cetyltrimethylammonium bromide (C16), dodecyltrimethylammonium bromide (C12), and fan-shaped 3,4,5-tris(dodecyloxy)benzenamine (Ar-3C12) were selected to form ionic supramolecular complexes with PSPAS and PSPCS, as illustrated in Scheme 2, following the method described in the literature.⁸ The Ar-3C12 molecule was synthesized according to the reported method.²⁶ For the complexation with C12 and C16, the concentrations of surfactants in water were lower than the critical micelle concentration. In order to improve the dispersion of the surfactants in water, the solutions were heated at 60 °C for 5 h under

stirring. For the complexation with Ar-3C12, the cationic dendritic ammonium amphiphile was dissolved in THF (pH = 2–3 adjusted with HCl, with a concentration of 10 mg/mL). All complexation experiments were carried out at a stoichiometric ratio of the negative sulfonate and the positive ammonium groups. Taking PSPAS as an example, the polymer was dissolved in water (1 mg/mL) at 60 °C and stirred for 5 h, and the solution was then added into the surfactant solution under an intense stirring. The surfactant solution immediately became turbid, indicating the formation of complexes. In order to remove the unbound polyelectrolytes and surfactants in PSPAS-C12 and PSPAS-Ar-3C12, the raw products were redissolved in ethanol and THF and reprecipitated in a large excess of water and water/THF (2/1, v/v) sequentially. Finally, pure complexes were obtained after two dissolution–precipitation cycles. However, PSPAS-C16 was directly used for the characterization without further purification due to its poor solubility in organic solvents. The procedures for preparing PSPCS-C12, PSPCS-C16, and PSPCS-Ar-3C12 were similar to those for preparing PSPAS complexes. All complexes obtained were dried at 35 °C for 72 h before characterization.

RESULTS AND DISCUSSION

Synthesis and Characterization of Monomers and MJLCPEs. The monomers were synthesized according to Scheme 1. The structures of the monomers were confirmed by conventional analyses, including ^1H NMR, ^{13}C NMR, elemental analysis, and mass spectrometry. The two monomers were easily polymerized via the conventional radical polymerization method in aqueous solutions. For SPAS, the viscosity increased significantly and formed a gel during polymerization when polymerized in pure water, which could be attributed to the hydrogen bonding between water and PSPAS. Hence, DMF/ H_2O was used in order to decrease the viscosity of the system. The resultant polymers PSPAS and PSPCS were water-soluble because of their ionic nature.

The values of η_{sp}/c (viscosity/concentration) of PSPAS (1 mg/mL) and PSPCS (1 mg/mL) in aqueous solutions were 6.4 and 9.2 dL/g, respectively. The weight-average molecular

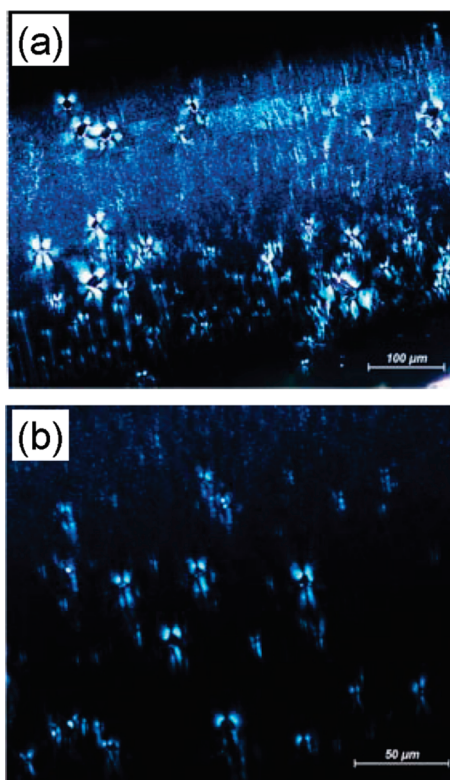


Figure 1. Polarized light micrographs of PSPAS (a) and PSPCS (b) in the solid state.

weight (M_w) of PSPAS was about 1.1×10^6 g/mol, and the polydispersity index (PDI) was 2.64, as determined by laser light scattering (LLS) at 25 °C in water with the addition of KCl to screen out the electrostatic interactions. The value of the absolute M_w of PSPAS determined by LLS demonstrated good polymerizability of the monomer SPAS. However, LLS could not be used to characterize PSPCS which had the ester linkage due to aggregation of PSPCS in the KCl solution. We speculated that the difference in the applicability of LLS in characterizing PSPAS and PSPCS was caused by the difference in the linkage in the side chains. The amide linkage was more hydrophilic than the ester one, and therefore, PSPAS was more soluble in aqueous solution.

Structures of MJLCPEs in Bulk. PLM, SAXS, and 2D WAXD results allowed a detailed analysis of the structures of the MJLCPEs. In the PSPAS and PSPCS solutions, no birefringence was observed by PLM. During the evaporation of water, gelation occurred. Birefringence was observed when a shear stress was applied to the gel-like samples by sliding the cover glass plates. The textures of the PSPAS and PSPCS in the solid state at ambient temperature shown in Figure 1 indicated the formation of ordered structures in PSPAS and PSPCS films.

SAXS experiments were carried out to determine their structures. About 10 mg of the MJLCPE was dissolved in water and cast onto a glass substrate, and then water was allowed to evaporate at ambient temperature. The samples were directly used for SAXS experiments without any further treatment. Figure 2 shows the SAXS profiles of PSPAS and PSPCS. The introduction of the sodium sulfonate group induced the strong segregation between the hydrophobic rigid cores and the hydrophilic end groups, which was reflected in the SAXS patterns with a first-order sharp peak centered at $q_1 = 3.08 \text{ nm}^{-1}$ along with a

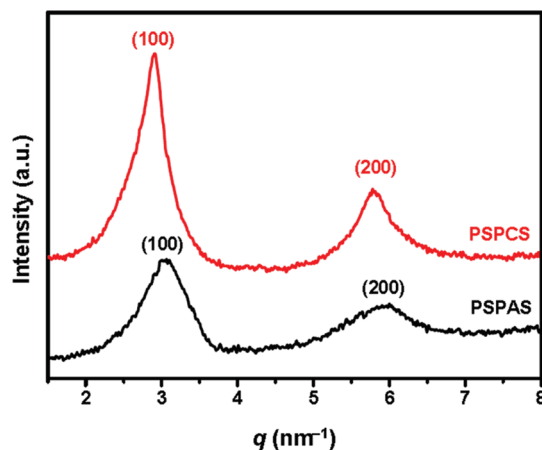


Figure 2. SAXS profiles of PSPAS and PSPCS bulk samples at ambient temperature, with intensity in log scale.

higher-order diffraction peak at $q_2 = 5.96 \text{ nm}^{-1}$ for PSPAS. The ratio of the scattering vectors of the two peaks $q_1:q_2$ was approximately 1:2, indicating a smectic structure with a periodicity of 2.04 nm ($d_{100} = 2\pi/q_1$) for PSPAS. PSPCS had the similar structure with the first peak appearing at a q value of 2.88 nm^{-1} , revealing the periodicity of 2.18 nm. These two layer spacing values were close to the calculated lengths of the monomers (1.82 nm, without considering the size of the sodium ion), which indicated that the side chains were perpendicular or almost perpendicular to the main chain, as in our previous packing models of smectic phases formed by MJLCPEs.²⁰

To identify the smectic structures of the two polymers, 2D WAXD experiments were carried out. Taking PSPAS as an example, the sample was put on the sample stage, and the point-focused X-ray beam was aligned normal to the film (Figure 3a). Figure 3b shows the pattern of PSPAS. Low-angle diffraction arcs appeared on the equator, and second-order diffractions also appeared on the equator. The scattering vector ratio of the two diffractions was 1:2, which was consistent with the SAXS result shown in Figure 2, as expected. In the high-angle region, the scattering halo was more or less concentrated on the meridian. The pattern in Figure 3b proved that the smectic phase of PSPAS was smectic A (S_A). Similar patterns were obtained from PSPCS samples, suggesting that PSPCS also formed an S_A phase (Figure 3c).

On the basis of SAXS and 2D WAXD results, we proposed the packing model sketched in Figure 4. Because of the strong segregation between the end groups and the rigid cores and the repulsion between the ionic end groups, the smectic phases were formed for the two MJLCPEs. The polymers took a more sheetlike conformation to pack into the smectic structures. Comparison with poly{2,5-bis[(4-methoxyphenyl)oxycarbonyl]-styrene} (PMPCS), which is different from PSPCS only in end groups but exhibits columnar phases,²⁷ indicated that the ionic interactions in PSPCS played an important role in generating the S_A phase, confirming again that strong side-chain interactions in MJLCPEs favored smectic phases.

Characterization on Ionic Complexes. Electrostatic complexation of rigid polyelectrolytes and flexible surfactants offers a facile way to tune the physical properties of polymers. The first indication of the complex formation was the change in solubility of the complexes comparing with solubilities of the polyelectrolytes

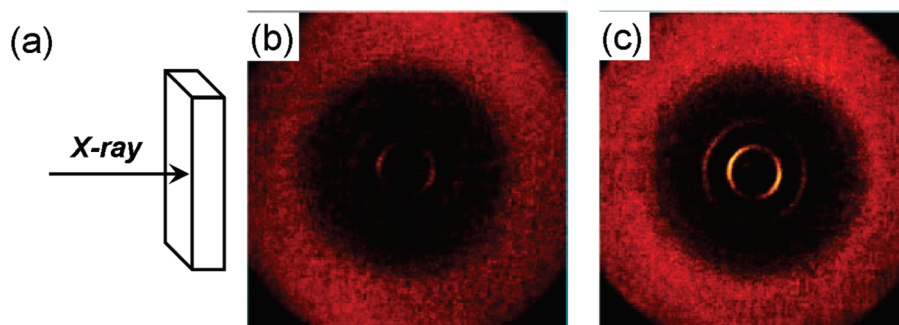


Figure 3. Schematic of the geometry in 2D WAXD experiments with the X-ray incident beam normal to the film (a) and 2D WAXD patterns of PSPAS (b) and PSPCS (c). Note that the equator and meridian directions are arbitrary.

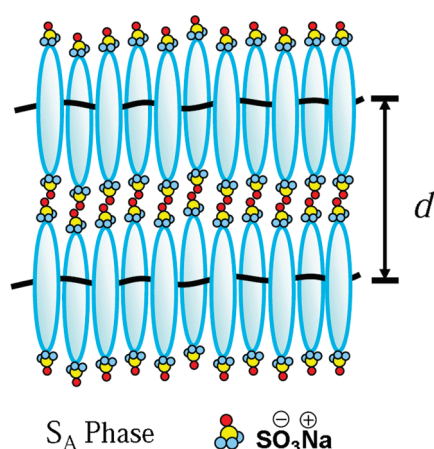


Figure 4. Schematic representation of the S_A phases of PSPAS and PSPCS polymers with sulfonate end groups.

and surfactants. For PSPAS-C12 and PSPCS-C12, the MJLCPEs and the surfactant C12 were all water-soluble, while the PSPAS-C12 and PSPCS-C12 precipitates survived several washing steps in water to remove unbound surfactant and polymers, indicating that the resultant precipitates could be the corresponding complexes instead of polymer/surfactant blends. ¹H NMR results also provided the evidence of electrostatic complexation between PSPAS and C12. Figure 5 shows the ¹H NMR spectra of the C12 surfactant and the complex PSPAS-C12 in methanol-*d*₄. The resonance peak at 3.14 ppm in the spectrum of C12 and that at 2.93 ppm in the spectrum of PSPAS-C12 corresponded to the methyl protons of the $-\text{N}(\text{CH}_3)_3$ group.²⁸ The upfield chemical shift for PSPAS-C12, owing to the fact that the sulfonate group shielded the protons of the methyl groups attaching to the quaternary ammonium following the complex formation, indicated the electrostatic interactions between the anionic polyelectrolyte and the cationic surfactant.²⁹ Compared with C12, the spectrum of the complex PSPAS-C12 showed an increase in widths of the resonance peaks, implying reduced mobility of the surfactant in the complex due to the attachment of C12 to PSPAS.²⁹

FTIR experiments were carried out to further prove the complex formation in bulk. The surfactants, the MJLCPEs, and their supramolecular complexes were characterized individually by FTIR. As an example, the spectra of C12, PSPAS, and PSPAS-C12 are shown in Figure 6a. The asymmetric and symmetric stretching vibration bands of the characteristic SO₃⁻ group in PSPAS were found at about 1190 and 1039 cm⁻¹, respectively.^{30,31}

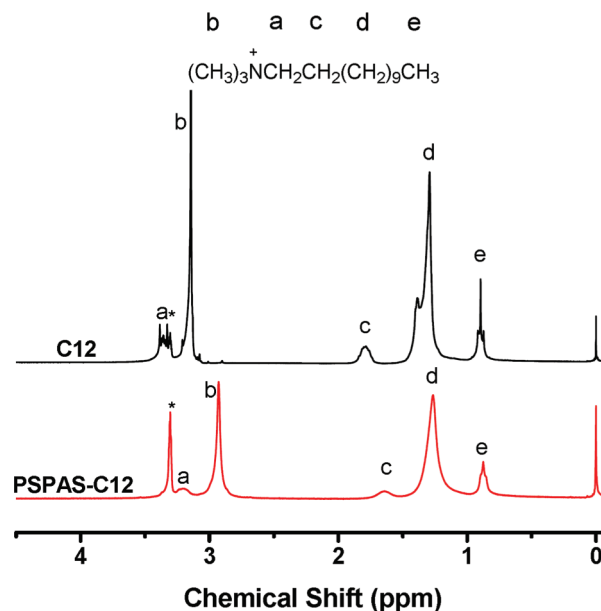


Figure 5. ¹H NMR spectra of C12 and PSPAS-C12. The asterisk indicates the signal of CH₃OH.

When PSPAS complexed with C12, the doublet vibration at ~1200 (1189 and 1216 cm⁻¹) appeared. The splitting of the asymmetric stretching vibration was related to the different electrostatic interaction strengths of the ionic pairs with N⁺—(CH₃)₃ and Na⁺.³¹ The vibration band at around 1473 cm⁻¹, which could be assigned to the CH₂ scissoring mode for C12,³² was present in the spectrum of PSPAS-C12 complex but absent in that of PSPAS. These results could prove the complexation between the sulfonate groups of PSPAS and the ammonium groups of C12. The similar phenomenon was also observed in spectra of PSPAS-C16 and PSPAS-Ar-3C12. Compared with C12, there was a benzene ring in Ar-3C12, which was demonstrated by the increased area of the C=C stretching vibration of benzene ring centered around 1595 cm⁻¹ in the spectrum of PSPAS-Ar-3C12 (Figure 6b) in comparison with that of PSPAS-C12. The spectrum of PSPAS-Ar-3C12 showed a larger splitting of the asymmetric stretching vibration compared with that of PSPAS-C12, indicating stronger electrostatic interactions in ionic pairs of SO₃⁻/N⁺—H₃ compared with those in SO₃⁻/N⁺—(CH₃)₃.³³ When the polyelectrolyte was changed to PSPCS, as demonstrated by FTIR spectra, the similar behavior was found for PSPCS-C12, PSPCS-C16, and PSPCS-Ar-3C12.

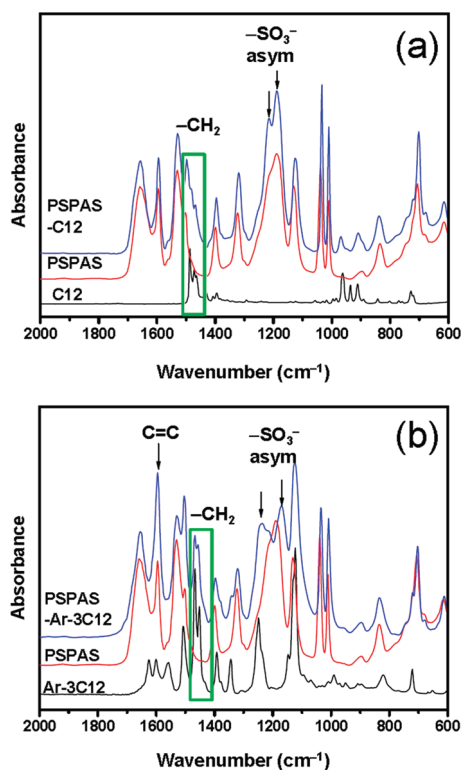


Figure 6. Infrared spectra in the 600–2000 cm^{-1} region: C12 surfactant, PSPAS polymer, and PSPAS-C12 complex (a); Ar-3C12 surfactant, PSPAS polymer, and PSPAS-Ar-3C12 complex (b).

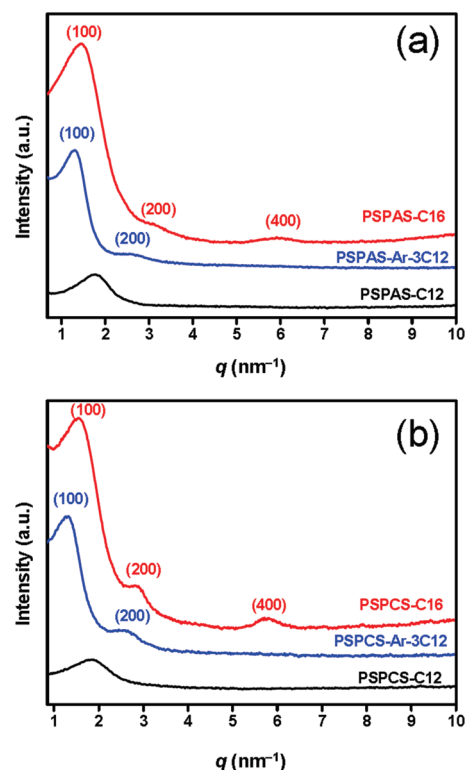


Figure 7. SAXS profiles of PSPAS (a) and PSPCS (b) polymers complexed with C12, C16, and Ar-3C12 surfactants at ambient temperature, with intensities in log scale.

Table 1. Elemental Analysis and SAXS Results of the MJLCE Complexes

sample	c (wt %) ^a	neutralization degree x (mol % surfactant) ^b	layer spacing d (nm) ^c	mesophase
PSPAS-C12	61.0	52.3	d	
PSPAS-Ar-3C12	66.8	48.5	4.79	lamellar
PSPAS-C16	62.2	47.6	4.33	lamellar
PSPCS-C12	58.9	36.5	d	
PSPCS-Ar-3C12	67.3	53.9	4.79	lamellar
PSPCS-C16	60.7	38.2	4.19	lamellar

^a Obtained from elemental analysis. ^b Calculated from C content. ^c Values of d_{100} from SAXS profiles. ^d Birefringent under PLM.

In order to calculate the composition of the complexes, elemental analysis was carried out. The composition was deduced from the C content in the complex. The results are summarized in Table 1. It could be found that substoichiometric complexes were obtained, although the experiments were carried out at a stoichiometric ratio of the anionic sulfonate and the cationic ammonium groups. Because of the poor solubility of the resultant complexes, they would precipitate out even when a fraction of the surfactants was bound onto the polymers. It was a challenge to find a good solvent which could dissolve the surfactants, polymers, and complexes at the same time. On the other hand, due to the steric hindrance and the high density of the ionic groups in the polyelectrolytes, it was difficult to reach

the complete protonation. However, the composition of each complex was in the region of 40–50%, which made it easier to characterize the complexes at the similar level of neutralization degree (x).

SAXS experiments were used to identify the types of liquid crystalline phases of these complexes. Parts a and b in Figure 7 show two sets of SAXS profiles of PSPAS and PSPCS complexed with C12, C16, and Ar-3C12 surfactants at ambient temperature, respectively. In order to clearly show multiple reflections, the intensities were plotted in log scale. Taking the complexes of PSPAS as an example, in the case of PSPAS-C12, only a single broad peak was present in Figure 7a, indicating that the system was poorly ordered, although it showed birefringence under PLM. The d -spacing of the broad peak corresponding to the average chain-to-chain distance was 3.47 nm, which was much larger than the chain-to-chain distance of 2.04 nm for PSPAS discussed above, indicating that the surfactant indeed acted as a relatively long spacer between PSPAS backbones in the complex. However, judging from the lack of higher-order peaks in the SAXS profile, the flexible content in the C12 surfactant was not enough to stabilize an ordered packing of the complex. The phenomenon was similar to the case of the polymers formed from a dendronized polymer (PG1) and the C8 surfactant, where the amorphous state was also observed because of the short alkyl chains.^{7,8}

By using the C16 surfactant with a longer alkyl tail, the microphase separation between the polar polybases and the nonpolar alkyl chains resulted in the formation of ordered structures, which could be attributed to the increased volume fraction of the flexible component. This was reflected in the SAXS profile of PSPAS-C16 in Figure 7a, with three diffraction

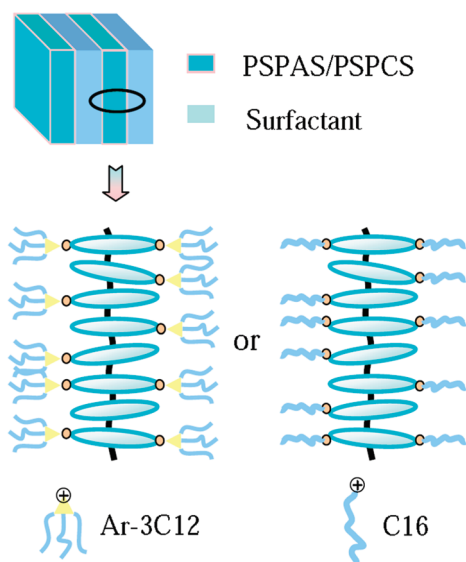


Figure 8. Schematic representation of lamellar phases of PSPAS-Ar-3C12 (PSPCS-Ar-3C12) and PSPAS-C16 (PSPCS-C16) complexes, formed by the addition of surfactants to MJLCPEs.

peaks having a scattering vector ratio of 1:2:4, which was typical of a lamellar phase with a larger d -spacing of 4.33 nm.

When a fan-shaped amphiphile Ar-3C12 with a polar head at the tip of the fan and three C12 nonpolar tails was used, two diffraction peaks could be observed in the SAXS profile of the complex in Figure 7a, with a scattering vector ratio of 1:2, indicating a lamellar phase having a larger d -spacing of 4.79 nm. The lack of even higher-order diffractions indicated the poorer ordering of PSPAS-Ar-3C12 compared with that of the PSPAS-C16 complex. On the one hand, the increase in the volume fraction of the alkyl tails had a pronounced consequence on the microphase separation. On the other hand, the length of the rigid side chains was increased by the introduction of the benzene ring in Ar-3C12. From our previous study,²⁰ smectic phases could be induced by extending the length of the mesogenic side chain. Consequently, the lamellar phase was obtained for PSPAS-Ar-3C12. However, the fan shape of the Ar-3C12 surfactant might have caused some difficulty in packing of the complex, leading to a poorer ordering of PSPAS-Ar-3C12.

The similar behavior was also observed for the PSPCS-C12, PSPCS-C16, and PSPCS-Ar-3C12 complexes, which was demonstrated in Figure 7b. The layer spacing values of the complexes are listed in Table 1. Furthermore, there was no distinct difference in the type of mesophases between the complexes formed by PSPAS and PSPCS. Because electrostatic interactions had much larger bond strength than hydrogen bonding,³ the linkage in the side chains did not have a significant effect on the phase structures of the complexes. On the basis of SAXS results and composition data of the complexes, a schematic drawing of the molecular packing of the ionic complexes between PSPAS and PSPCS with C16 and Ar-3C12 surfactants is depicted in Figure 8. However, due to the difficulty in obtaining oriented samples, whether the lamellar structures were S_A -type or smectic C-type could not be determined. It is worth noting that all ordered ionic complexes here were obtained directly from the precipitates without any further treatment, which could be attributed to the strong electrostatic interactions in the complexes and the self-assembling nature of MJLCPEs.

CONCLUSIONS

In summary, we synthesized a new series of water-soluble MJLCPEs containing the amide or ester linkage in the side chains via conventional radical polymerization. Both polymers formed smectic A phases in bulk after the evaporation of water from the cast solutions. The liquid crystalline behavior of the nonstoichiometric complexes between the polyelectrolytes and surfactants depended on the length and shape of the surfactants. Our results indicated that the LC structures of the complexes were not affected by the different linkages in the side chains of the two polyelectrolytes because the electrostatic interactions played a dominant role in determining the structures. The complexes were amorphous when the MJLCPEs were complexed with C12 because the alkyl tails were too short to induce the formation of ordered LC structures. However, by increasing the length of the alkyl tails as in C16 or by changing the shape of surfactant as in the fan-shaped amphiphilic molecule with three C12 tails (Ar-3C12), lamellar phases were observed for the complexes. In addition, we have demonstrated that MJLCPE–surfactant complexes could be easily synthesized through electrostatic interactions, which provided a green and simple method to construct new functional MJLCPEs.

ASSOCIATED CONTENT

S Supporting Information. Details about the laser light scattering experiments on PSPAS and the results. This material is available free of charge via the Internet at <http://pubs.acs.org>.

AUTHOR INFORMATION

Corresponding Author

*E-mail: fanhx@pku.edu.cn (X.-H.F.); zshen@pku.edu.cn (Z.S.); zhumpf@dhu.edu.cn (M.-F.Z.).

ACKNOWLEDGMENT

Financial support from the National Natural Science Foundation of China (Grants 50925312, 50973016, 20974002, and 20990232) and the Programme of Introducing Talents of Discipline to University (No. 111-2-04) is gratefully acknowledged.

REFERENCES

- (1) Kato, T. *Science* **2002**, *295*, 2414–2418.
- (2) Faul, C.; Antonietti, M. *Adv. Mater.* **2003**, *15*, 673–683.
- (3) Pollino, J. M.; Weck, M. *Chem. Soc. Rev.* **2005**, *34*, 193–207.
- (4) Ober, C. K.; Wegner, G. *Adv. Mater.* **1997**, *9*, 17–31.
- (5) Chen, Y.; Shen, Z.; Gehringer, L.; Frey, H.; Stiriba, S. E. *Macromol. Rapid Commun.* **2006**, *27*, 69–75.
- (6) Canilho, N.; Scholl, M.; Klok, H.-A.; Mezzenga, R. *Macromolecules* **2007**, *40*, 8374–8383.
- (7) Canilho, N.; Kasëmi, E.; Mezzenga, R.; Schlüter, A. D. *J. Am. Chem. Soc.* **2006**, *128*, 13998–13999.
- (8) Canilho, N.; Kasëmi, E.; Schlüter, A. D.; Mezzenga, R. *Macromolecules* **2007**, *40*, 2822–2830.
- (9) Kristen, N.; von Klitzing, R. *Soft Matter* **2010**, *6*, 849–861.
- (10) Thüemann, A. F. *Prog. Polym. Sci.* **2002**, *27*, 1473–1572.
- (11) Pace, G.; Tu, G.; Fratini, E.; Massip, S.; Huck, W. T. S.; Baglioni, P.; Friend, R. H. *Adv. Mater.* **2010**, *22*, 2073–2077.
- (12) Coppin, C. M.; Leavis, P. C. *Biophys. J.* **1992**, *63*, 794–807.
- (13) Kornyshev, A. A.; Lee, D. J.; Leikin, S.; Wynveen, A. *Rev. Mod. Phys.* **2007**, *79*, 943.
- (14) Boddohi, S.; Kipper, M. J. *Adv. Mater.* **2010**, *22*, 2998–3016.

- (15) Yun, H. C.; Chu, E. Y.; Han, Y. K.; Lee, J. L.; Kwei, T. K.; Okamoto, Y. *Macromolecules* **1997**, *30*, 2185–2186.
- (16) Yang, W.; Furukawa, H.; Shigekura, Y.; Shikinaka, K.; Osada, Y.; Gong, J. P. *Macromolecules* **2008**, *41*, 1791–1799.
- (17) Every, H. A.; Mendes, E.; Picken, S. J. *J. Phys. Chem. B* **2006**, *110*, 23729–23735.
- (18) Viale, S.; Best, A. S.; Mendes, E.; Jager, W. F.; Picken, S. J. *Chem. Commun.* **2004**, 1596–1597.
- (19) Wong, G. C. L. *Curr. Opin. Colloid Interface Sci.* **2006**, *11*, 310–315.
- (20) Chen, X.-F.; Shen, Z.; Wan, X.-H.; Fan, X.-H.; Chen, E.-Q.; Ma, Y.; Zhou, Q.-F. *Chem. Soc. Rev.* **2010**, *39*, 3072–3101.
- (21) Chen, S.; Gao, L. C.; Zhao, X. D.; Chen, X. F.; Fan, X. H.; Xie, P. Y.; Zhou, Q. F. *Macromolecules* **2007**, *40*, 5718–5725.
- (22) Gopalan, P.; Andruzzi, L.; Li, X.; Ober, C. K. *Macromol. Chem. Phys.* **2002**, *203*, 1573–1583.
- (23) Cheng, Y.-H.; Chen, W.-P.; Shen, Z.; Fan, X.-H.; Zhu, M.-F.; Zhou, Q.-F. *Macromolecules* **2011**, *44*, 1429–1437.
- (24) Zhang, D.; Liu, Y.-X.; Wan, X.-H.; Zhou, Q.-F. *Macromolecules* **1999**, *32*, 5183–5185.
- (25) Chattopadhyay, G.; Chakraborty, S.; Saha, C. *Synth. Commun.* **2008**, *38*, 4068–4075.
- (26) Lincker, F.; Bourgun, P.; Masson, P.; Didier, P.; Guidoni, L.; Bigot, J.-Y.; Nicoud, J.-F.; Donnio, B.; Guillon, D. *Org. Lett.* **2005**, *7*, 1505–1508.
- (27) Ye, C.; Zhang, H.-L.; Huang, Y.; Chen, E.-Q.; Lu, Y.; Shen, D.; Wan, X.-H.; Shen, Z.; Cheng, S. Z. D.; Zhou, Q.-F. *Macromolecules* **2004**, *37*, 7188–7196.
- (28) Kreke, P. J.; Magid, L. J.; Gee, J. C. *Langmuir* **1996**, *12*, 699–705.
- (29) Macdonald, P. M.; Tang, A. *Langmuir* **1997**, *13*, 2259–2265.
- (30) Yang, J. C.; Mays, J. W. *Macromolecules* **2002**, *35*, 3433–3438.
- (31) Atorngitjawat, P.; Runt, J. *Macromolecules* **2007**, *40*, 991–996.
- (32) Venkataraman, N. V.; Vasudevan, S. *J. Phys. Chem. B* **2001**, *105*, 1805–1812.
- (33) Chen, W.; Sauer, J. A.; Hara, M. *Polymer* **2003**, *44*, 7729–7738.